

CHARACTERIZATION OF PORE STRUCTURE OF FILTRATION MEDIA

Akshaya Jena and Krishna Gupta

Porous Materials, Inc.

83 Brown Road, Ithaca, NY 14850

ABSTRACT

The principles of extrusion flow porometry, extrusion porosimetry, mercury intrusion porosimetry, non-mercury intrusion porosimetry and gas adsorption techniques used for pore structure characterization of filtration media are briefly outlined. Pore structure characteristics measurable by these techniques are illustrated with examples and are interpreted. The strengths, limitations and operational features of the techniques are compared. The advantages of using multiple techniques are considered.

KEYWORDS

Characterization techniques. Pore structure. Pore diameter. Pore distribution. Pore volume. Permeability. Surface area. Flow Porometry. Porosimetry. Gas adsorption.

INTRODUCTION

Filtration media in various forms including woven cloths, nonwovens, membranes and particulate beds are used extensively in a wide variety of applications in areas such as biotech, health care, pharmaceutical, food and beverage, power sources and chemical industries. The performance of filtration media in all of these industries is determined by the pore structure characteristics of the media. Three kinds of pores are normally found in materials (Figure 1). The closed pores are not accessible. The blind pores terminate within the material. The through pores permit fluid flow through the material and, hence, are the relevant pores for this application. The important pore structure characteristics of filter media are the most constricted through pore diameter, the largest pore diameter, the mean pore diameter, pore shape, pore distribution, pore volume, pore volume distribution, surface area, liquid permeability, gas permeability and influence of operational parameters such as compressive stress, cyclic compression, pressure, temperature, chemical environment, sample orientation, inhomogeneity and layered or graded structures.



Figure 1: Closed, blind and through pores in materials.

Various techniques are available to measure the pore characteristics. However, no one technique can measure all the properties. Also, the same property is often measured differently by different techniques. In this paper, available techniques are briefly outlined, the significance of quantities measured by these techniques are analyzed, the strengths of the techniques are compared and the advantage of using multiple techniques has been pointed out.

TECHNIQUES

Two kinds of techniques can be used for pore structure characterization. The microscopic techniques include methods like high-resolution light and electron microscopy and x-ray scattering. These techniques examine tiny areas, which may not be representative of macroscopic areas of interest for applications. Also none of the flow properties is determinable. The techniques are involved, time consuming and expensive. The macroscopic techniques scan large sample areas of interest in applications. These are based on particle challenge, liquid extrusion, liquid intrusion, and gas adsorption. In the particle challenge test, particles of known size are allowed to pass through the sample. The test can yield pore size and distribution, but cannot give the flow properties. This test is also time consuming and expensive. The liquid extrusion, liquid intrusion and gas adsorption techniques can measure a variety of properties, are inexpensive and can be fast. Therefore, these techniques and their derivatives (Figure 2) are widely used in applications.

Macroscopic Techniques			
Particle Challenge	Liquid Extrusion	Liquid Intrusion	Gas Adsorption
	1. Extrusion Flow Porometry	1. Mercury Intrusion Porosimetry	1. Vapor Adsorption
	2. Extrusion Porosimetry	2. Non-mercury Intrusion Porosimetry	2. Vapor Condensation

Figure 2. Macroscopic techniques for pore structure characterization of filtration.

media.

EXTRUSION FLOW POROMETRY (CAPILLARY FLOW POROMETRY)

In this technique, a wetting liquid is used to fill the pores of the sample. For a wetting liquid, liquid/solid surface free energy ($\gamma_{l/s}$) is less than the solid/gas surface free energy ($\gamma_{s/g}$). Therefore, filling of the pores is spontaneous, but removal of the liquid from the pores is not. Pressure of a non-reacting gas on the sample is increased to remove the wetting liquid from pores and permit gas flow. For the gas pressure to be adequate to displace liquid in a pore, the work done by the gas must be equal to the increase in surface free energy.

$$p \, dV = (\gamma_{s/g} - \gamma_{l/s}) \, dS \quad (1)$$

where p is differential pressure, dV is increase in volume of gas in pore, and dS is increase in solid/gas surface area and the corresponding decrease in solid/liquid

surface area (Jena and Gupta 2001). In terms of wetting liquid surface tension, γ , and contact angle, θ (Figure 3):

$$\gamma_{lv} - \gamma_{sl} + \gamma \cos \theta = 0 \quad (2)$$

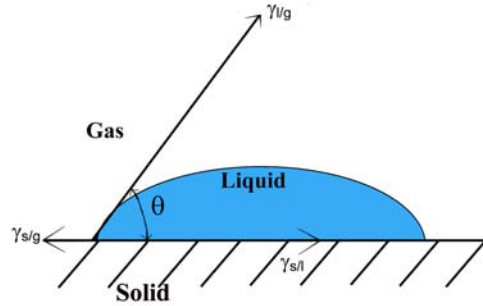


Figure 3. Relation between contact angle and surface tensions.

The pore cross-sections of filtration media can be quite complex and the pore size may be unspecific. The diameter of a pore at any location along its path is defined as the diameter, D of a cylindrical opening that has the same (dS/dV) as the pore. At the location of interest.

$$\begin{aligned} (dS/dV)_{\text{pore}} &= (dS/dV)_{\text{cylindrical opening of diameter, } D} \\ &= 4/D \end{aligned} \quad (3)$$

The relation between pore diameter and the differential pressure required to displace the wetting liquid in the pore is obtained from Equations 1, 2 & 3:

$$p = 4 \gamma \cos \theta / D \quad (4)$$

This equation suggests that the largest pore is emptied first and higher pressures are required to empty smaller pores (Figure 4).

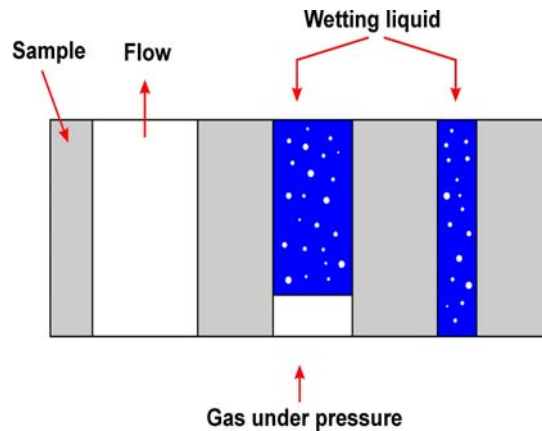


Figure 4. Principle of capillary flow porometry.

The flow meters detect the presence of pores by sensing increase in flow rate at a given applied differential pressure due to emptying of pores at that applied differential pressure. Differential pressures and flow rates through wet and dry samples are measured (Figure 5). These measured differential pressures and flow rates are used to evaluate the most constricted through pore diameters, the largest pore diameter, the mean flow pore diameter, flow distribution over pore size, gas permeability, external surface area, average particle diameter and average fiber diameter. Measurement of volume of displaced liquid due to application of differential pressure on excess liquid maintained on the sample allows computation of liquid permeability.

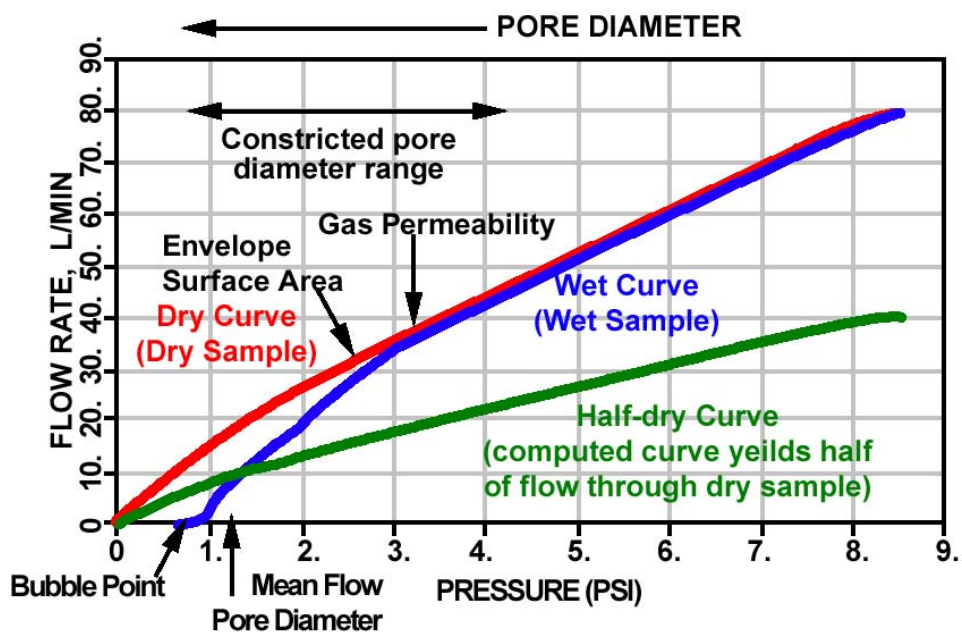
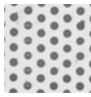
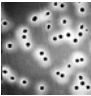


Figure 5: Typical results of capillary flow porometry obtained using a nanofiber filtration medium (1 psi = 6.8947 kPa).

Many fully automated models of flow porometer are commercially available. Instruments based on flow porometry can give highly reproducible and accurate data (Gupta and Jena 1999. Mayer 2002). Pore diameters of etched cylindrical pores measured by flow porometry are in excellent agreement with those directly measured in SEM (Jena and Gupta 2001). Table I shows typical results.

Table I. Pore diameters of pores measured by SEM and flow porometry.

Sample	SEM Micrograph	Pore diameter, μm	
		SEM	PMI Porometer
Etched stainless steel disc		81.7 ± 5.2	86.7 ± 4.1
Polycarbonate membrane		4.5 ± 0.5	4.6 ± 0.1

EXTRUSION POROSIMETRY

In this technique, the sample is placed on a membrane whose largest pore is smaller than the smallest pore of interest in the sample. A liquid that wets the sample and the membrane is used to spontaneously fill all the pores of the sample and the membrane. A pressurized non-reacting gas is used to remove liquid from pores of the sample (Figure 6). The differential gas pressure required to displace the wetting liquid in the pore is given by Equation 4. However, pressure used to remove liquids from pores of the sample is not sufficient to remove liquid from pores of the membrane because these pores are smaller than the pores in the sample (Equation 4). Consequently, liquid displaced from pores of the sample passes through the membrane while the pores of the membrane remain filled with the liquid and prevent gas to pass through (Jena and Gupta 2002).

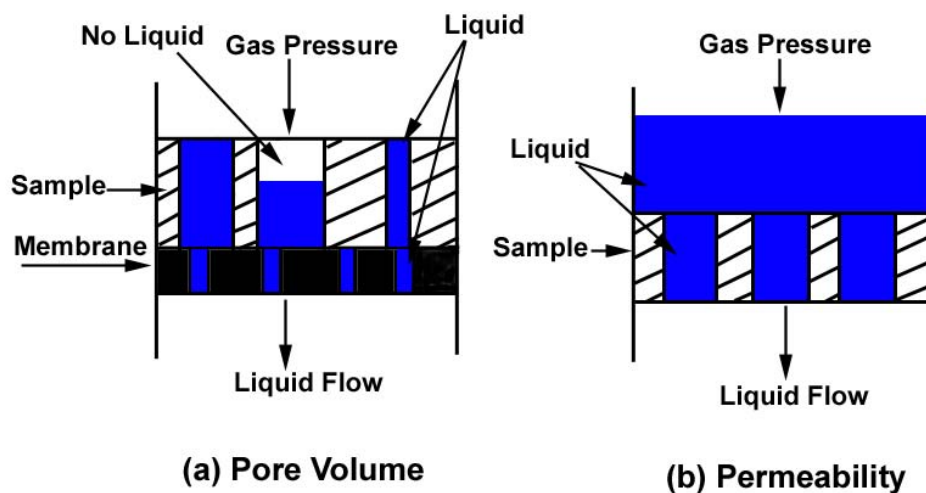


Figure 6: Principle of extrusion porosimetry

The differential gas pressure and volume of extruded liquid are measured. These data (Figure 7) are used to calculate pore volume, pore volume distribution and surface area of through pores. Removal of the membrane and measurement of volume of displaced liquid as a function of time due to pressure on excess liquid maintained on the sample after removal of the membrane permit computation of liquid permeability (Figure 6).

Extrusion porosimeters are commercially available. Custom instruments with several options for liquid volume measurement techniques are also available.

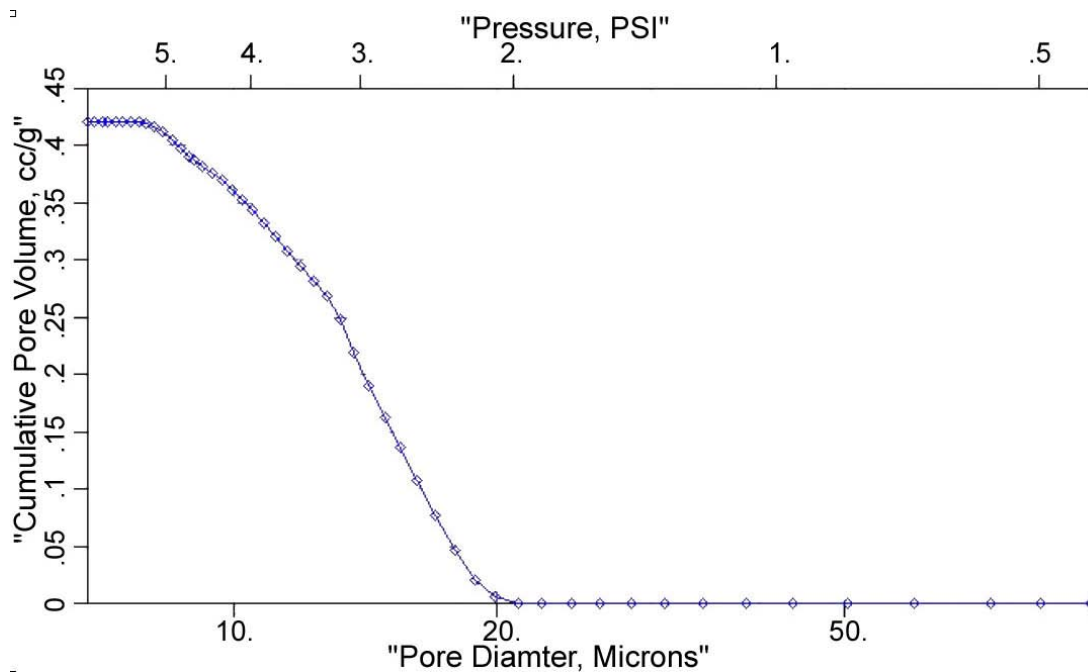


Figure 7: Typical results from a hydrogel using extrusion porosimetry.

MERCURY INTRUSION POROSIMETRY

For a non-wetting liquid, liquid/solid interfacial free energy is higher than the gas/solid interfacial free energy and the contact angle is greater than 90°. When a sample is surrounded by a non-wetting liquid, it does not flow spontaneously into the pores of the sample. Increased pressure on the non-wetting liquid forces it into the pores of the sample.

Pressure required to intrude a non-wetting liquid into a pore is obtained by equating the work done by forcing the liquid into pore to the increase in surface free energy. Using the relation between contact angle and surface tension in Equation 2 and the definition of pore diameter in Equation 3:

$$p = - 4 \gamma \cos \theta / D \quad (5)$$

Mercury is non-wetting for most materials. Measured differential pressure on mercury and the intrusion volume of mercury are measured. The acquired data are similar to those in Figure 7. The measured values are used to compute pore volume, pore diameter, pore volume distribution, and surface area of through and blind pores (Lowell and Shields 1984).

A variety of models of mercury intrusion porosimeters are commercially available. Models with minimum mercury exposure are also available.

NON-MERCURY INTRUSION POROSIMETRY

This technique is exactly the same as mercury intrusion porosimetry, except that instead of mercury a non-wetting non-mercury liquid is used for intrusion. Water and oil are some of the non-mercury intrusion liquids that are often used. In this technique, no toxic material is used, liquid used in the application can often also be the test fluid, the pressures are low and the smaller pore sizes are normally measurable. Custom non-mercury intrusion porosimeters can satisfy the needs of the user.

GAS ADSORPTION TECHNIQUE

When a clean surface is exposed to a gas an adsorbed film forms on the surface and the extent of adsorption is determined by the temperature, pressure and the nature of the gas. In the gas adsorption technique, the amount of vapor adsorbed on the pore surface of a sample is measured as a function of pressure of vapor below the equilibrium vapor pressure. The data are analyzed using BET theory to compute surface area (Lowell and Shields 1984).

$$\left[\frac{p}{(p_0 - p)W} \right] = \left[\frac{1}{W_m C} \right] + \left[\frac{(C-1)}{W_m C} \right] \left(\frac{p}{p_0} \right) \quad (6)$$

where p is vapor pressure, p_0 is equilibrium vapor pressure at the temperature of measurement, W is the amount of adsorbed gas, W_m is amount of gas that can form a monolayer and C is a constant. When vapor pressure is low, $[0.05 \leq (p/p_0) \leq 0.35]$

variation of $[p/(p_0 - p)W]$ with (p/p_0) is linear and the slope and the intercept of the best straight line yields W_m . Typical results for a filtration media are shown in Figure 8.. The surface area of through and blind pores is computed using the following relation.

$$S = W_m N \alpha / m \tag{7}$$

where S is the surface area per unit mass, W_m is in moles, N is the Avogadro's number, α is the cross-sectional area of an adsorbed molecule and m is the mass of the sample.

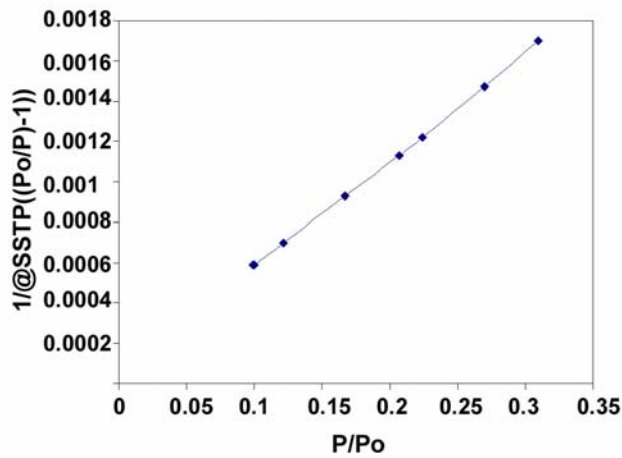


Figure 8: Linear variation of $[p/(p_0 - p)W]$ with (p/p_0) for a filtration medium.

At high relative vapor pressure, (p/p_0) , vapor tends to condense in pores.

Condensation of vapor at $p < p_0$ into liquid is accompanied by increase in free energy and filling of pores with liquid results in replacement of high free energy vapor/solid interface by the low free energy liquid/solid interface. The relation between pore

size and vapor pressure is obtained by equating the two energy terms. Let liquid, l , of volume dV condense in a pore from vapor, $v(p)$, at pressure, p , and the resulting conversion of the solid/vapor interfacial area to solid/liquid interfacial area be dS .

Hence:

$$(dV / \underline{V}) \Delta G [v(p) \rightarrow l (\text{bulk})] + dS \Delta G^s [s/v \rightarrow s/l] = 0 \quad (8)$$

where \underline{V} is the specific volume of liquid, ΔG is the free energy change due to condensation and ΔG^s surface free energy change. In terms of equilibrium vapor pressure, p_o , of the liquid and the surface free energies:

$$\Delta G [v(p) \rightarrow l (\text{bulk})] = \Delta G [v(p) \rightarrow v(p_o)] = RT \ln (p_o / p)$$

$$\Delta G^s [s/v \rightarrow s/l] = (\gamma_{sl} - \gamma_{sv})$$

From these relations, the relation between surface tension and contact angle in Equation 3 and the definition of pore diameter in Equation 3:

$$\ln (p/p_o) = - [4 \underline{V} \gamma \cos \theta / RT] / D \quad (9)$$

where R is the gas constant and T is the absolute temperature.

Equation 9 suggests that with increase of vapor pressure, vapor condenses in larger pores.

The relative vapor pressure and the amount of vapor condensed in pores are measured as functions of vapor pressure. Through and blind pore diameters are

computed from vapor pressure and pore volume is computed from volume of condensed vapor (Lowell and Shields 1984). Variation of pore volume with pore diameter is similar to that shown in Figure 7. Such data are used to compute pore volume distribution.

Many models of gas adsorption instruments are commercially available. The simple ones are table top models capable of measuring surface area quickly. The sophisticated models may have multiple sample chambers and are capable of measuring surface area, pore diameter, pore volume, adsorption/desorption isotherms and chemisorption using a variety of gases.

MEASURABLE PORE STRUCTURE CHARACTERISTICS

Pore diameter

Measurable pore diameter: A pore normally has many diameters because the diameter of a pore changes considerably along pore path; each part of a pore has a well defined pore diameter. Each technique tends to measure a different pore diameter.

Let us consider the through pore in Figure 9. Flow porometry detects the presence of this pore by sensing the gas flow through the pore. The gas pressure for displacement of liquid in the pore (Figure 9) is a maximum at the most constricted part of the pore. Until this pressure is reached, the gas displaces liquid in the pore up to the most constricted part. At the maximum pressure, the remaining liquid in the pore beyond the most constricted part is removed, the pore becomes completely empty, the gas flows through the pore and the flow meter detects the pore by sensing increase in flow rate. Thus, the pressure at which flow is detected

corresponds to the pressure required for liquid displacement at the most constricted part of the pore and the measured pore diameter is the diameter of the pore at its most constricted part (Figure 9). Thus, flow porometry measures the most constricted pore diameters of only the through pores.

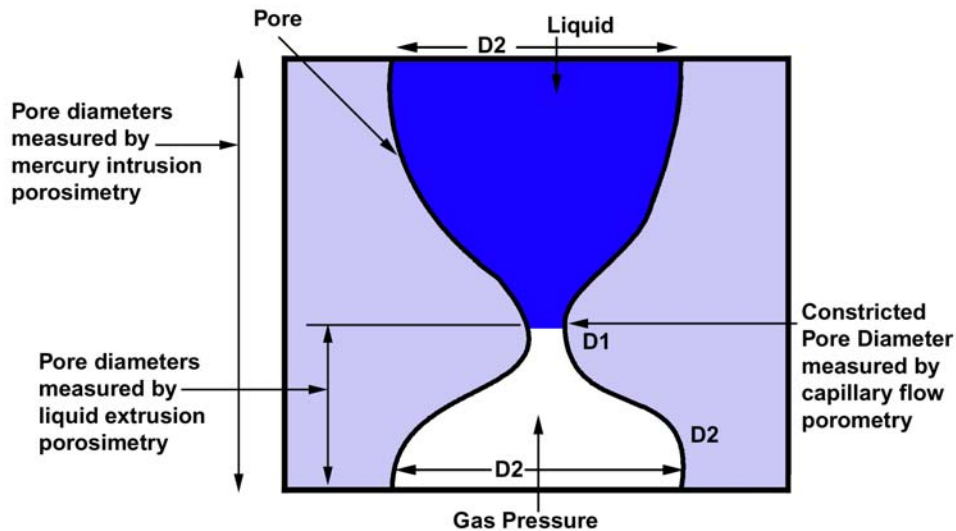


Figure 9: Pore diameters of a constricted pore measured by different techniques.

With increase in gas pressure on one side of the sample tested by extrusion porosimetry, the gas displaces the liquid in the pore and the pore diameter and volume of that part of the pore in which liquid is displaced, are measured. However, on attaining the maximum pressure at the most constricted part of the pore, the gas displaces the rest of the liquid from the pore beyond the most constricted part and the diameters of the part of the pore beyond the most constricted part are not measured (Figure 9). Thus, extrusion porosimetry measures pore diameters of that part of a pore between the entry point of the gas and the most constricted point in the pore (Figure 9). This technique measures diameters of only the through pore.

In mercury intrusion as well as non-mercury intrusion porosimetry, the non-wetting liquid enters the pore (Figure 9) from both sides. With increasing pressure the liquid enters smaller parts of the pore and the pore diameter and volume of those parts are measured until the most constricted part is filled with the liquid. Thus, a range of pore diameters of all parts of a through pore is measured (Figure 9). Pore diameters and volumes of blind pores are also measured by this technique because the liquid can enter the pore from the open side. However, the diameter of a part of a blind pore is not measurable if it is larger than its diameter at the entry point of the pore. In the gas adsorption technique, condensation occurs in narrow parts at low pressures and with increasing pressure condensation occurs in wider parts. Thus, pore diameters of all parts are measured (Figure 9). However, these three techniques, mercury porosimetry, non-mercury porosimetry and gas adsorption technique measure diameters of both the through pores and blind pores.

The most constricted, the largest most constricted and the mean flow most constricted through pore diameters: Such pore diameters control the barrier properties of the filtration media used for separation of particles from fluids. Flow porometry is the only technique that is capable of determining the most constricted pore diameters.

Differential pressures measured in flow porometry give the most constricted pore diameters. The pressure required to initiate flow through the wet sample is known as the bubble point pressure. The largest most constricted through pore diameter is calculated from the measured bubble point pressure using Equation 4.

The mean flow pore diameter is computed from the mean flow pressure, which corresponds to the intersection of the wet curve with the half-dry curve. The half-dry curve is a calculated curve that yields half of the flow rate through the dry sample. The mean flow pore diameter is such that half of the flow is through pores larger than the mean flow pore and the other half of the flow is through pores smaller than the mean flow pore. The mean flow pore diameter is a measure of permeability (Mayer 2002). The data in Figure 5 yield the following values.

The most constricted through pore diameter range: 1.5 – 8 μm .

The largest most constricted through pore diameter: 10.237 μm .

The mean flow most constricted through pore diameter: 5.038 μm .

Multiple diameters of through pores: The diameters of through pores between the entry point of the gas and the most constricted point of the pore are measured by extrusion porosimetry. Thus a range of pore diameters for each pore is measured. (Figure 7).

Multiple diameters of through and blind pores: Intrusion porosimetry and gas adsorption techniques give pore diameters of all parts of through and blind pores. As a result, pore diameters of wide mouth pores measured by these three techniques are normally higher than those measured by flow porometry.

Range of measurable pore diameters: Each technique has a range over which the pore diameters are accurately measurable. Table II lists the approximate measurable range.

Table II: Pore diameter and pore volume normally measurable by various techniques.

Techniques	Pore diameter range, μm	Minimum pore volume, cm^3
Extrusion		
Flow Porometry:	0.013 – 500	--
Extrusion		
Porosimetry:	0.1 – 2000	0.0001
Mercury Intrusion		
Porosimetry:	0.03 – 200	0.0001
Non-Mercury Intrusion		
Porosimetry:	0.001 – 20	0.0001
Gas Adsorption:	0.0005 – 2	0.0001

Pore diameters not measurable: The pore structure of filtration media is usually very complex. In a complex structure, many of the pore diameters may not be measurable. A few examples are considered here in order to illustrate the problem. If the pore configuration is such that wider parts of through pores are accessed by narrow parts, the diameters of wider parts are not measurable by any one of the techniques except gas adsorption (Figure 10a). When wide through pores are connected by narrow pores, the diameters of narrow pores are not measurable by flow porometry and extrusion porosimetry (Figure 10b), but can be measured by gas adsorption and intrusion porosimetry. Blind pores are not measurable by flow porometry and extrusion porosimetry (Figure 10c), but can be measured by gas adsorption and intrusion porosimetry. If the blind pores end in wide parts (Figure 10d), the diameters of wide parts are not measurable by any one of the techniques except gas adsorption.

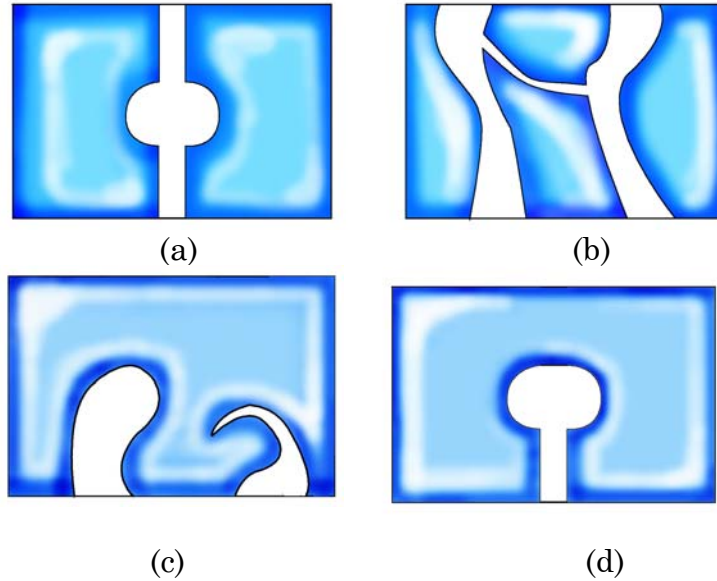


Figure 10. Possible complex pore configurations.

Flow distribution over through pore diameters

Gas flow distribution over pore diameter is a measure of gas permeability, rate of the process, liquid permeability and filter efficiency. Flow distribution is also related to pore fraction distribution (Jena and Gupta 1999). The flow distribution is expressed in terms of flow distribution function, f :

$$f = - [(d f_w / d f_d) \times 100 / d D] \quad (10)$$

where f_w and f_d are flow rates through wet and dry samples respectively at the same differential pressure. Capillary flow porometry is the only technique that can give the flow distribution. Figure 11 illustrates such a distribution for a filter material. The area under the curve in any pore size range is the percentage flow through that pore size range.

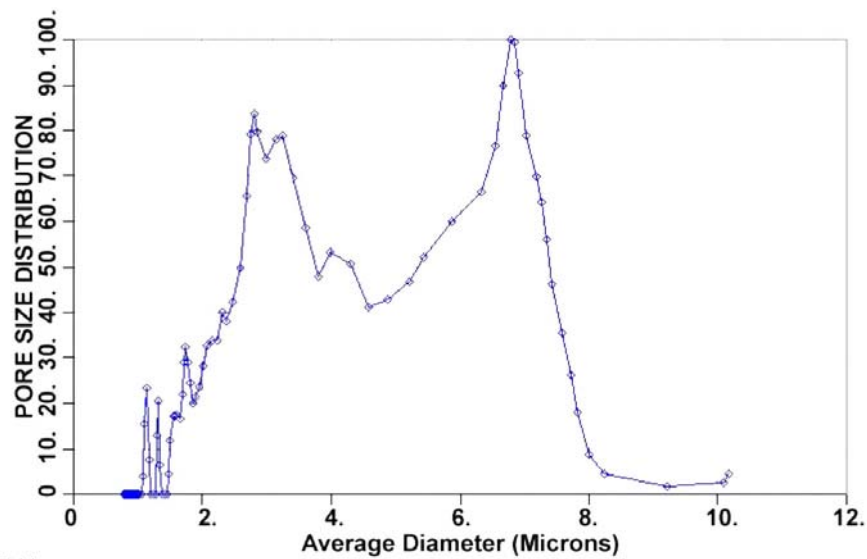


Figure 11 Gas flow distribution in a nonwoven filter material over pore diameter obtained using capillary flow porometry. The function is normalized by considering its maximum value to be one hundred percent.

Pore volume

All the techniques except flow porometry can measure pore volumes. However, each technique can accurately measure pore volume of certain kind of pore in a certain pore size range (Table 2). In the appropriate range, the results obtained by various techniques are comparable

Through pore volume: Extrusion porosimetry is the only technique that measures through pore volume (Figure 7).

Through and blind pore volume: Intrusion porosimetry and gas adsorption technique measure pore volume of through and blind pores. Blind pore volume may

be computed by subtracting from the volume of through and blind pores, the through pore volume. measured by extrusion porosimetry.

Closed pore volume: The total volume of through, blind and closed pores can be estimated from the true and bulk densities of the product. The volume of closed pores is the difference between the total pore volume and volume of through and blind pores.

Pore volume distribution

The pore volume distribution is given by the distribution function f_v :

$$f_v = - (dV/d \log D) \quad (11)$$

The function is such that in the plot of distribution function against $\log D$, the area under the curve in any pore diameter range gives the volume of pores in that pore diameter range. Because different techniques measure different pore diameters and different kinds of pores, the volume distributions measured by different techniques are not comparable.

The distribution functions for volume and flow for the through pore in Figure 9 is shown in Figure 12. The flow distribution shows only one flow rate corresponding to one pore diameter (the most constricted pore diameter). Pore volume distribution by mercury intrusion, non-mercury intrusion and gas adsorption typically are close. However, the distribution by extrusion porosimetry tends to show a higher volume associated with the constricted pore diameter.

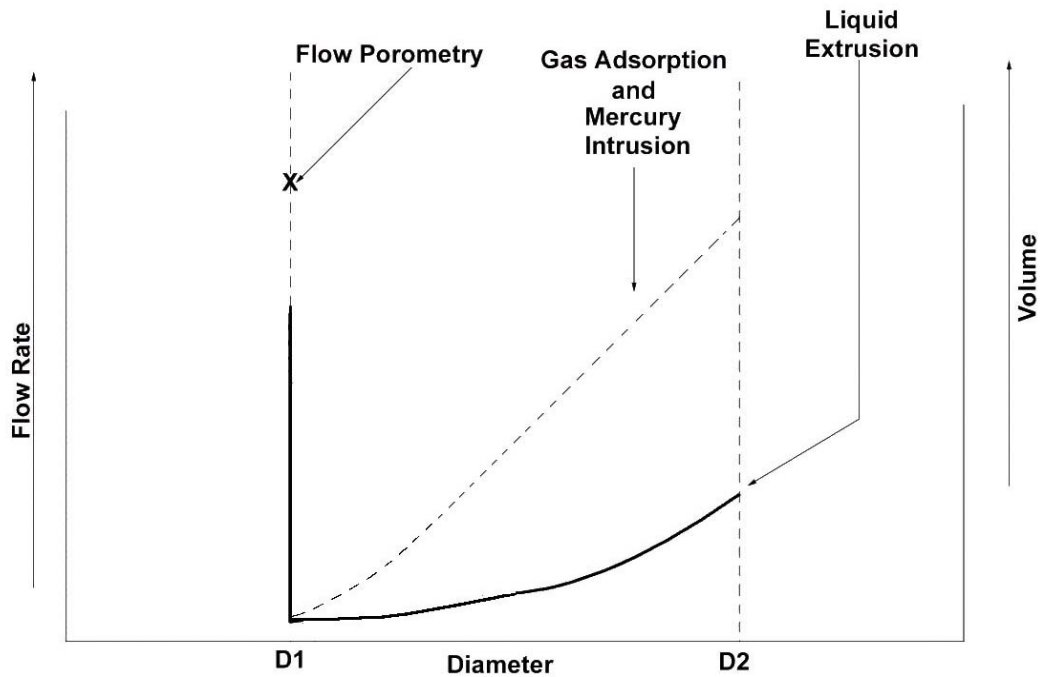


Figure 12 Distribution for the single pore in Figure 9.

Distribution of through and blind pore volume is obtained by the intrusion techniques and gas adsorption. Presence of blind pores tends to shift these distributions relative to the distribution measured by extrusion porosimetry. An example is shown in Figure 13.

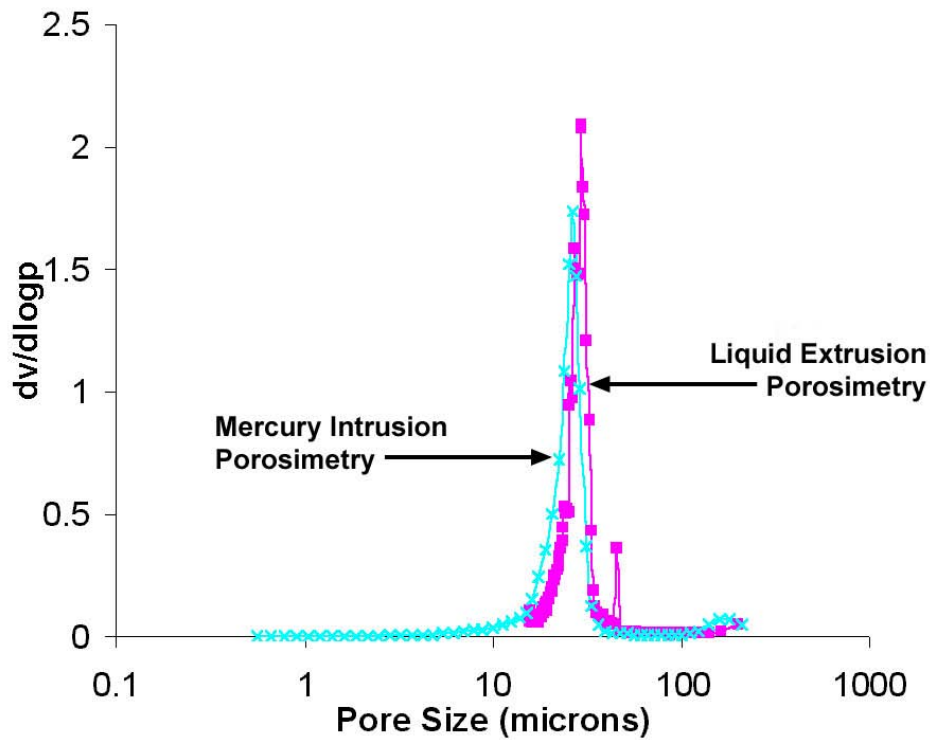


Figure 13: Pore volume distribution of a ceramic filter by mercury intrusion porosimetry and extrusion porosimetry showing shift of distribution due to blind pores.

Surface area

Through and blind pore surface area: Surface area of through and blind pores can be measured accurately by gas adsorption using Equation 7. The surface area of through and blind pores can also be estimated from the variation of pore volume with pore diameter measured by intrusion techniques.

$$S = \int [4/D] dV \tag{12}$$

The computed values are often less accurate because of large integration errors introduced by large changes in pressure due to small changes in volume. Pores like ink-bottle shaped blind pores can introduce considerable error. For example, intrusion porosimetry measures pore volume of an ink-bottle pore to be associated with a pore of diameter equal to the diameter of the neck of the pore. Therefore, the surface area is over estimated.

Through pore surface area: Through pore surface area can be measured both by extrusion porosimetry and flow porometry. Equation 12 is used to compute surface area from variation of through pore volume measured by extrusion porosimetry. The surface area is also computed from gas flow rates measured by flow porometry using Kozeny-Carman relation between flow rate and external surface area (Kraus, Ross and Girifalco, 1953). The results obtained by this technique agree well with the results of gas adsorption for materials that are essentially free from blind pores. The results obtained with a nonwoven illustrate the excellent agreement in Table III.

Table III: Surface area of a nonwoven.

Technique	Surface area,
Flow porometry	0.56 m ² /g
Gas adsorption	0.52 m ² /g

Gas Permeability

According to Darcy's law, flow of fluids through porous media is proportional to the pressure gradient causing flow (Carman 1956). The proportionality constant is normally a function of the viscosity of the fluid. Therefore, incorporating viscosity in the equation, Darcy's law becomes:

$$\underline{F} = k (A / \mu l) (p_i - p_o) \tag{13}$$

where \underline{F} is the volume flow rate at the average pressure per unit time, k is permeability, μ is viscosity of the fluid, A is cross-sectional area of the porous material, l is the thickness of the porous material, p_i is inlet pressure and p_o is outlet pressure. Thus permeability can be computed from measured flow rates and differential pressures. Many simple instruments are available for just permeability measurement. However, amongst the five techniques that are capable of performing multiple tests, flow porometry is the only technique that is capable of measuring gas permeability. Gas flow rate measured through dry sample yields gas permeability. Flow porometer is a versatile instrument that can measure gas permeability of a variety of gases over a wide range of pressures and temperatures. Figure 14 shows air permeability through a filtration media as a function of temperature. Permeability can be expressed in any desired unit like m^2 , Darcy, Frazier, Gurly and Rayle.

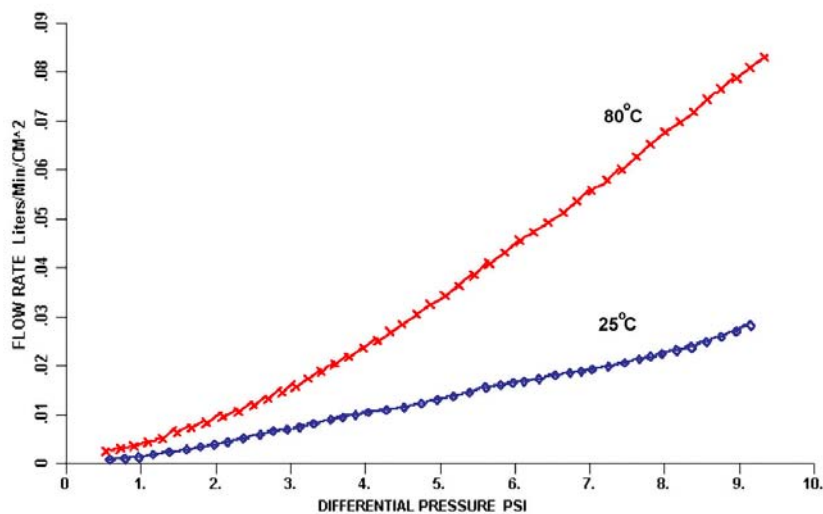


Figure 14: Air permeability of a filtration media at two temperatures.

Liquid permeability

Liquid permeability is computed from measured liquid flow rates and differential pressures using Equation 13. Many simple instruments are available for just liquid permeability measurement. However, amongst the five techniques that are capable of performing multiple tests, the flow porometry and extrusion porosimetry are the only techniques that are capable of measuring liquid permeability. Flow porometer measures liquid flow rate using a penetrometer, when pressure is increased on excess liquid maintained on the sample in the porometer. The extrusion porosimeter measures liquid flow rate under similar conditions when the membrane is removed from underneath the sample. These are versatile instruments, which can measure liquid permeability of a variety of strong chemicals at elevated temperatures and high pressures. Thus, permeability under true service conditions may be evaluated (Jena and Gupta 2002). Figure 15 illustrates data obtained on permeability for a 30 % KOH solution.

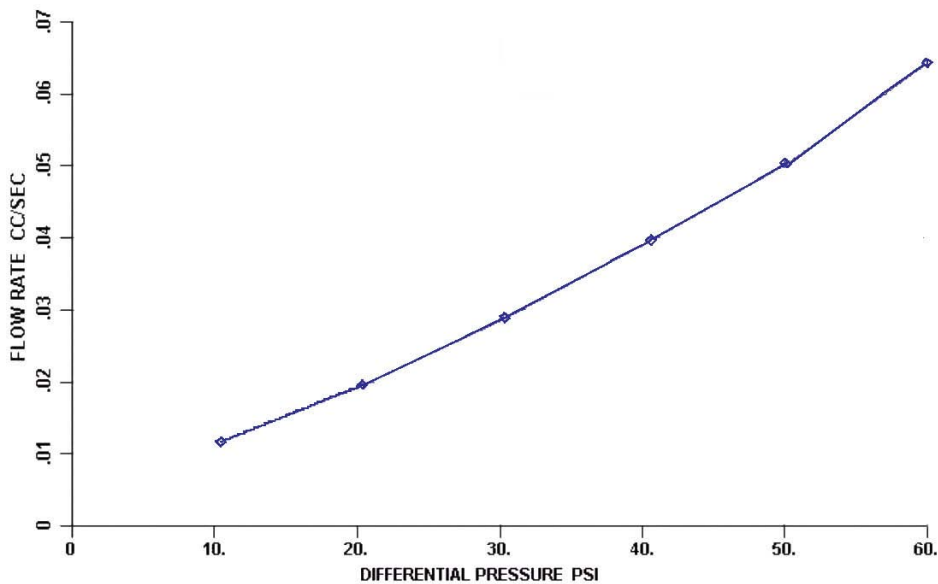


Figure 15: Permeability of 30% KOH solution.

Homogeneity of pore structure

Filtration media produced in large volumes can be quite inhomogeneous (Jena and Gupta 2002). Testing at multiple locations required for evaluation of homogeneity may result in unacceptable damage to the material and may be time consuming. Techniques are now available to test a material at any desired location in-situ (Jena and Gupta 2002). Figure 16 shows a porometer with a mobile test head that can be clamped on to any test location on filtration media.

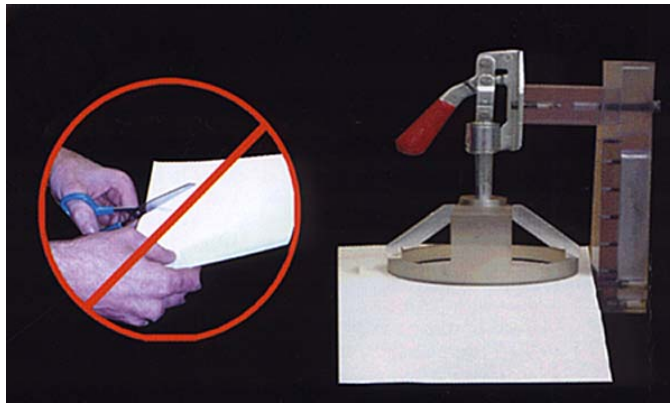


Figure 16. Porometer that does not require samples to be cut from test materials.

Pore structure in the x-y plane

The characterization techniques do not distinguish between pore characteristics in different directions in a porous material, although for many applications differences between the pore size and distribution in the thickness direction and those in the x-y plane of a porous material has considerable effect on performance. In-plane porometers are capable of measuring pore diameters and pore size distributions along the thickness direction (z-direction) as well as in the x-y plane (Jena and Gupta 2000). Pore structure of a number of materials can be

considerably different in the two directions (Perna and Jena 1999). For example, the ratio of the through-plane and in-plane bubble points in thin wrapping paper is 27.4, whereas, in thick transmission fluid filter felt the ratio is 1.86.

Pore structure of graded or multi-layered media

Many efficient filter media are either multi-layered, graded or coated. Such unusual pore structures can be analyzed using available test equipment. Pore characteristics of individual layers of multi-layer materials can be characterized in-situ without separating the layers in a in-plane flow porometer (Jena and Gupta 2002). Pore structures of coatings and supported membranes can be analyzed in a porometer using a combination of through-plane and in-plane tests (Jena and Gupta 2001). The orientation of graded pores can be established using extrusion porosimetry (Jena and Gupta 2002). The considerably different pore distributions in the two layers of a hot gas filtration medium measured in-situ in a porometer is reproduced in Figure 17.

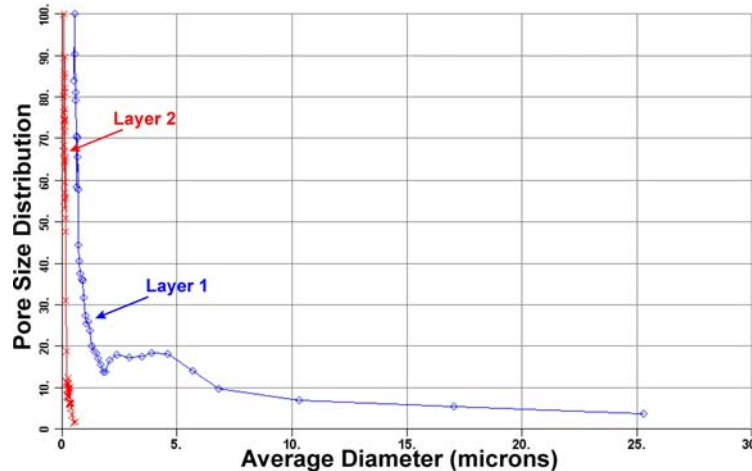


Figure 17. Pore distributions in the two layers of a hot gas filtration medium measured in-situ in a porometer.

Effect of service conditions on pore structure

Pore structures of filter materials are normally determined at ambient conditions. However, the filter material may operate under stress, at elevated temperatures, in chemical environments, at high pressures and under cyclic stress. The pore structure under such actual service conditions needs to be evaluated because of their relevance to applications.

The flow porometer is versatile enough to permit tests to be carried out under simulated service conditions. Effects of cyclic stress, compressive stress, temperature, pressure and chemical environment on pore structure of filtration media can be determined using flow porometry. As an example, the effect of compressive stress on the largest pore diameter in a filter is shown in Figure 18 (Gupta and Jena 1999). In this figure the ratio of the largest pore diameter, D , under compressive stress, σ , and the largest pore diameter under zero stress, D_0 , is plotted against σ^2 . In this case, the effect of stress is too large to be ignored.

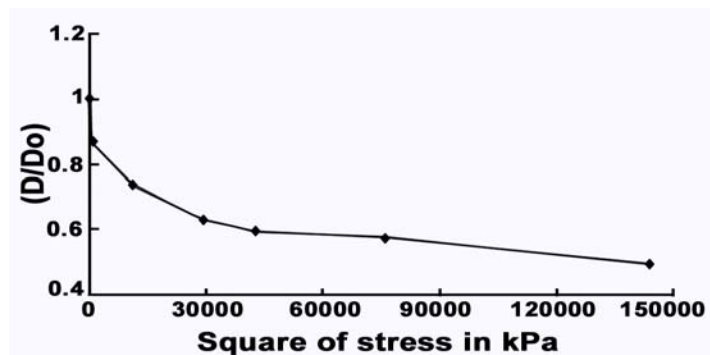


Figure 18. Effect compressive stress on the largest pore diameter.

Liquid extrusion porosimetry is another technique, which can measure effects of compressive stress, temperature and pressure on pore volume. However, the other techniques are incapable of measuring the effects of service conditions on pore structure characteristics of filtration media.

COMPARISON OF TECHNIQUES

The abilities of the techniques for pore structure characterization are summarized in Table IV. In this table \checkmark means the property is measurable by the technique and \times means the property is not measurable by the technique. Table V lists the operational features of the techniques. In this table \checkmark means yes and \times means no. It is clear that each technique has its strengths and certain limitations.

Table IV: Capabilities of the techniques

Property	Extrusion flow porometry	Extrusion porosimetry	Intrusion porosimetry (mercury)	Intrusion porosimetry (non-mercury)	Gas adsorption
Through pores					
Constricted diameter	\checkmark	\times	\times	\times	\times
Largest Constricted diameter	\checkmark	\times	\times	\times	\times
Many diameters of each pore	\times	\checkmark	\times	\times	\times
Flow distribution	\checkmark	\times	\times	\times	\times
Volume	\times	\checkmark	\times	\times	\times
Volume distribution	\times	\checkmark	\times	\times	\times
Surface area	\checkmark	\checkmark	\times	\times	\times
Through and					

Blind Pores					
All diameters of each pore	×	×	√	√	√
Volume	×	×	√	√	√
Volume distribution	×	×	√	√	√
Surface area	×	×	√	√	√
Permeability					
Gas permeability	√	×	×	×	×
Liquid permeability	√	√	×	×	×
Effects of application environment					
Compressive stress	√	√	×	×	×
Cyclic compression	√	×	×	×	×
Strong chemical environment	√	√	×	×	×
Elevated Temperature	√	√	×	×	×
High pressure	√	×	×	×	×
Layered structure	√	×	×	×	×
Orientation	√	×	×	×	×

Table V. Operational Features.

Features	Extrusion flow porosimetry	Extrusion porosimetry	Intrusion porosimetry (mercury)	Intrusion porosimetry (non-mercury)	Gas adsorption
Use of toxic material	×	×	√	×	×
High pressure	×	×	√	×	×
Subzero Temperature	×	×	×	×	√
Use of fluid of interest	√	√	×	√	×
Involved / time consuming	×	√	√	×	√

USE OF MULTIPLE TECHNIQUES

No single technique can measure all the pore structure characteristics. Therefore, multiple techniques used for examination of a material can yield considerably more information about pore structure. This is illustrated by data in Table VI obtained for a ceramic filtration medium using extrusion flow porometry, extrusion porosimetry and intrusion mercury porosimetry (Jena and Gupta 2002). A sketch of possible pore structure is illustrated in Figure 19.

Table VI. Pore structure characteristics of ceramic filtration media.

Through pores	
The constricted largest pore diameter:	450.4 μm .
The average constricted pore diameter:	3.867 μm
Constricted pore diameter range:	450.4 - 0.39 μm
Average of all pore diameters	18 μm
Volume:	1.982 cm^3/g ,
Percent of total pore volume:	79.5 %
Surface area:	0.43 m^2/g
Percent of total surface area:	5 %
Shape:	Pores with 4 μm constrictions and >18 μm mouth
Blind Pores	
Diameter of wide parts:	> 18 μm
Diameter of narrow parts:	\approx 0.02 μm .
Volume:	0.51 cm^3/g
Percentage of total pore volume:	20.5 %
Surface area:	9.01 m^2/g
Percent of total surface area:	95 %
Shape:	Wide mouth with long narrow tails

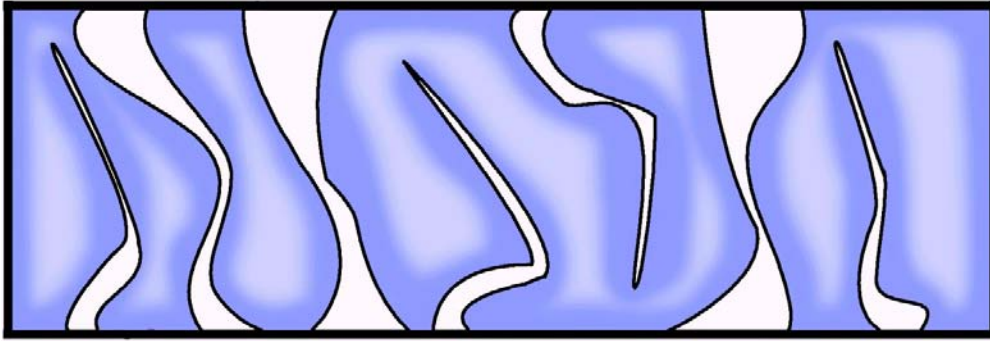


Figure 19. Sketch of the pore structure derived from data obtained by multiple test techniques.

SUMMARY AND CONCLUSION

1. Techniques available for characterization of pore structure of filtration media have been reviewed and measurable characteristics have been discussed.
2. The parameters determinable by these techniques have been critically examined and interpreted. It has been shown that the same characteristic measured by different techniques may not be comparable because the characteristics measured by different techniques have different significance.
3. With the use of modern, sophisticated instruments with high accuracy, it is now possible to determine pore characteristics such as effects of compression, cyclic compression, elevated temperature, pressure, strong chemical environment and orientation on pore structure and permeability.
4. The strengths, limitations and operational features of the techniques have been considered.

5. The value of the use of multiple techniques has been illustrated.

REFERENCES

Carman, P. C., Flow of Gases through Porous Media, Academic Press, 1956.

Gupta, Vibhor and Jena, A.K., 'Substitution of Alcohol in Porometers for Bubble Point Determination', Advances in Filtration and Separation Technology, American Filtration and Separation Society, Vol.13b, pp. 833-844, 1999.

Gupta, Vibhor and Jena, A.K., 'Effects of Compression on Porosity of Filter Materials', Advances in Filtration and Separation Technology, American Filtration and Separation Society, Vol.13a, pp. 10-17, 1999.

Jena, Akshaya and Gupta, Krishna, 'An Innovative Technique for Pore Structure Analysis of Fuel Cells and Battery Components using Flow Porometry', Journal of Power Sources, Vol. 96, pp. 214-19, 2001.

Jena, Akshaya and Gupta, Krishna, 'Accuracy and Reproducibility of Pore Size Determined by Flow Porometry, Presented at The 14th Annual Technical Conference, The American Filtration & Separation Society, May 1-4, 2001, Tampa, Florida.

Jena, Akshaya and Gupta, Krishna, 'Measurement of Pore Volume and Flow through Porous Materials', Materials Testing: MP Materialprufung, Jahrg. 44, pp.243-245, 2002.

Jena, A.K. and Gupta, K.M., 'Pore Size Distribution in Porous Materials', Proceedings of International Conference Filtration 99, November 3-4, Chicago, INDA, 1999.

Jena, Akshaya and Gupta, Krishna, 'Evaluation of Permeability of Strong Chemicals at Elevated Temperatures and High Pressures', The 2002 17th Annual Battery Conference on Applications and Advances, California State University, Long Beach, California, Proceedings, December 2002, IEEE Catalog Number 02TH8576.

Jena, Akshaya and Gupta, Krishna, 'Homogeneity of Pore Structure of Filtration Media', Proceedings of the 15th Annual Technical Conference, April 9-12, 2002, Galveston. Texas, The American Filtration & Separation Society, 2002.

Jena, Akshaya and Gupta, Krishna, 'In-Plane and Through-Plane Porosity in Coated Textile Materials', Journal of Industrial Textiles, Vol. 29, No. 4, pp.317-325, 2000.

Jena, A. and Gupta, K., 'Analyse der Porendurchmesser von Mehrschicht-Filtermitteln', F & S Filtrieren und Separieren, Jahrg. 16, No.1, pp. 13-17, 2002.

Jena, A. and Gupta, K., 'A Novel Technique for Characterization of Pore Structure of Ceramic Membranes', The Journal of the Filtration Society, Vol. 1 (4), pp. 23-26, 2001.

Jena, Akshaya and Gupta, Krishna, 'Use of Multiple Test Techniques for Evaluation of Complex Pore Structures' Proceedings of the 15th Annual Technical Conference, April 9-12, 2002, Galveston, Texas, American Filtration & Separation Society, 2002.

Kraus, Gerard, Ross, J. W. and Girifalco, L. A., 'Surface Area Analysis by Means of Gas Flow Methods'. I. Steady State Flow in Porous Media, Phys. Chem., Vol. 57. pp. 330-333, 1953.

Lowell, S. and Shields, E., Powder Surface Area and Porosity, Chapman Hall Publication, 1984.

Mayer, Ernest, 'Porometry Characterization of Filtration Media', Proceedings of the 15th Annual Technical Conference, The American Filtration & Separation Society, April 9-12, 2002, Galveston, Texas,

Perna, Vincent and Jena, A. K., 'In-Plane and Through-Plane Porosities in Nonwovens', Proceedings 1999, TAPPI Nonwovens Conference, March 15-17, Orlando, TAPPI Press, pp. 177- 187, 1999.